INTERNATIONAL JOURNAL OF
RADIATION ONCOLOGY • BIOLOGY • PHYSICS
www.redjournal.org

PHYSICS CONTRIBUTION

Normal Tissue Sparing by FLASH as a Function of Single-Fraction Dose: A Quantitative Analysis

Till Tobias Böhlen, PhD,* Jean-François Germond, PhD,* Jean Bourhis, MD, PhD,† Marie-Catherine Vozenin, PhD,† Esat Mahmut Ozsahin, MD, PhD,† François Bochud, PhD,* Claude Bailat, PhD,* and Raphaël Moeckli, PhD*

*Institute of Radiation Physics, Lausanne University Hospital and Lausanne University, Lausanne, Switzerland; and †Department of Radiation Oncology, Lausanne University Hospital and Lausanne University, Lausanne, Switzerland

Received Feb 2, 2022; Accepted for publication May 24, 2022

Purpose: The FLASH effect designates normal tissue sparing by ultra-high dose rate (UHDR) compared with conventional dose rate irradiation without compromising tumor control. Understanding the magnitude of this effect and its dependency on dose are essential requirements for an optimized clinical translation of FLASH radiation therapy. In this context, we evaluated available experimental data on the magnitudes of normal tissue sparing provided by the FLASH effect as a function of dose, and followed a phenomenological data-driven approach for its parameterization.

Methods and Materials: We gathered available in vivo data of normal tissue sparing of conventional (CONV) versus UHDR single-fraction doses and converted these to a common scale using isoeffect dose ratios, hereafter referred to as FLASH-modifying factors (FMF= $(D_{CONV}/D_{UHDR})|_{isoeffect}$). We then evaluated the suitability of a piecewise linear function with 2 pieces to parametrize FMF $\times$ D_{UHDR} as a function of dose D_{UHDR}.

Results: We found that the magnitude of FMF generally decreases (ie, sparing increases) as a function of single-fraction dose, and that individual data series can be described by the piecewise linear function. The sparing magnitude appears organ-specific, and pooled skin-reaction data followed a consistent trend as a function of dose. Average FMF values and their standard deviations were 0.95 ± 0.11 for all data <10 Gy, 0.92 ± 0.06 for mouse gut data between 10 and 25 Gy, and 0.96 ± 0.07 and 0.71 ± 0.06 for mammalian skin-reaction data between 10 and 25 Gy and >25 Gy, respectively.

Conclusions: The magnitude of normal tissue sparing by FLASH increases with dose and is dependent on the irradiated tissue. A piecewise linear function can parameterize currently available individual data series.

Introduction

Large single doses ($\gtrsim$5 Gy) administered within short overall delivery durations ($\lesssim$0.2 seconds) using ultra-high dose rates (UHDR) result in reduced damage to normal tissues while also retaining antitumor efficacy compared with doses delivered with conventional dose rates (CONV) on the scale of minutes.[1-6] This differential effect, referred to as the

Corresponding author: Raphaël Moeckli, PhD; E-mail: raphael.moeckli@chuv.ch

This research was partially funded by the ISREC Foundation from a Biltema donation and by the Fondation pour le Soutien de la Recherche et du Developpement de l'Oncologie (FSRDO).

Disclosures: none.

Data sharing statement: Research data are stored in an institutional repository and will be shared upon reasonable request to the corresponding author.

Supplementary material associated with this article can be found in the online version at doi:10.1016/j.ijrobp.2022.05.038.

Acknowledgments—The authors thank Drs Brita Singers Sørensen and Pierre Montay-Gruel, as well as Benoit Petit and Jonathan Ollivier, for sharing their data.

0360-3016/$ - see front matter
https://doi.org/10.1016/j.ijrobp.2022.05.038

FLASH effect, is receiving significant attention in the field of radiation therapy (RT), because dose-modifying factors for normal tissue sparing from 1.1 up to 1.8 have been reported and could be exploited to improve the therapeutic ratio.[1,3,6] Normal tissue sparing by the FLASH effect has now been confirmed by different institutes and for different beam modalities (electrons, photons, protons), species (mouse, rat, cat, mini pig, zebrafish), organs (brain, gastrointestinal tract, lung, skin), and endpoints (lethal dose, skin and gut reactions, neurologic tests), including early and late toxic effects.[1-5,7,8] All this has led recently to the treatment of the first human patient.[9] However, although the amount and quality of experimental data can be regarded as conclusive from an evidence perspective, the data are sparse from a quantitative and modeling perspective.

Understanding the magnitudes and dependencies of the FLASH effect on dose-delivery parameters (ie, dose, temporal beam delivery structure, and fractionation scheme) is an essential requirement for its successful clinical translation with an optimized therapeutic ratio, and may also contribute to a better understanding of its mechanism. Also, the sparing potential for different biologic systems and endpoints needs to be understood quantitatively. Several recent treatment planning studies have quantified the FLASH effect using binary yes/no threshold models,[10-13] resulting in discontinuous responses and, in the case of a yes/no threshold value for dose,[12,13] in a hormesis effect (ie, a small increase in dose over the threshold results in a decreased effect for the concerned normal tissue). These choices are mostly the result of the still-developing knowledge base for the FLASH effect, and underline the need for more quantitative descriptions backed by data and more systematic investigations of relevant dependencies. Several potential FLASH-effect mechanisms have been proposed but to date, none of these hypotheses has been validated.[2,6,14-24] Hence, while the mechanisms of the FLASH effect for normal tissues are under investigation, one can quantify basic dependencies of the magnitudes of the FLASH normal tissue-sparing effect by following a phenomenological top−down approach based on available experimental in vivo data, and assess current uncertainties in the prediction of the FLASH effect based on uncertainties of the experimental data used for such modeling.

Normal tissue complication probabilities (NTCP) for a given irradiated organ and volume depend primarily on the administered dose; thus, this work focused on quantifying the magnitude and behavior of normal tissue sparing by the FLASH effect as a function of single-fraction dose based on available experimental evidence. For this purpose, we gathered and reformatted available experimental in vivo data of the FLASH sparing effect for normal tissues, and expressed them in terms of isoeffect dose ratios on a common scale as a function of dose. In a second step, we parametrized subgroups of data using a phenomenological function derived from the sigmoidal response behavior typically observed for NTCP.

Methods and Materials

Definition of FLASH-modifying factor

Analogous to the definition of relative biological effectiveness for different radiation qualities,[25] the FLASH-modifying factor (FMF) for UHDR irradiations is defined as the ratio of doses that need to be administered at conventional dose rates (D_{CONV}) and UHDR (D_{UHDR}) to achieve an isoeffect for a given biologic system and endpoint:

$$FMF = \frac{D_{CONV}}{D_{UHDR}}\Big|_{isoeffect} \quad (1)$$

The FMF is the inverse of the dose-modifying factor, found in various publications about the FLASH effect.[1,3] An FMF value <1 corresponds to normal tissue sparing of UHDR compared with CONV irradiation; hence, normal tissue sparing by the FLASH effect increases when FMF decreases.

Using this concept with slightly changed naming convention (analogous to the one used for proton and ion beam therapy[25]), a dose D delivered with UHDR can be converted into an isoeffective FMF-weighted dose D_{FMF}, delivered at conventional dose rates, as follows:

$$D_{FMF} = FMF \cdot D \quad (2)$$

Derivation of FMF from experimental data

We performed a systematic literature review of published in vivo data that compare normal tissue responses of UHDR to CONV irradiations. We searched PubMed in October 2021 using the following query: FLASH AND ("radiotherapy" OR "radiation" OR "irradiation") for articles published in 2014 (ie, the year Favaudon et al[2] published their seminal article) and afterward. The query produced 903 results. We screened the query results manually for in vivo data of normal tissue responses to UHDR irradiations compared with CONV irradiations from which FMF values could be derived. To the best of our knowledge, we also added further data sets known to us that did not contain the term "FLASH" (ie, specifically older data sets published before 2014).

A report and record identification and screening flowchart based on Preferred Reporting Items for Systematic Reviews and Meta-Analyses (PRISMA)[26] is provided in Table E1. A study was included if the following criteria were fulfilled: (1) contained in vivo normal tissue data for both UHDR irradiations with a time-averaged dose rate (TADR) >40 Gy/second and CONV irradiations (TADR: 0.001-1 Gy/second); (2) normal tissue data for a clinically relevant functional endpoint (eg, survival, skin/lung reaction scores, necrosis, deformity, growth, neurocognitive tests) or endpoints with a direct link to functional outcome (ie, in practice, crypt survival); and (3) FMF values needed to be extractable from the data. We excluded data sets from 2

studies[27,28] that were obtained in tissues with artificially reduced oxygen concentration (by clamping or N_2 breathing), because tissue sparing of UHDR compared with CONV irradiation was reported in these studies to be completely suppressed in such anoxic/hypoxic conditions with all resulting FMF values effectively close to 1, even for high doses up to 80 Gy. Consequently, almost all analyzed in vivo data sets were obtained for physiological oxygen concentrations (physoxic).[29] The properties of the 27 identified data sets are summarized in Table 1.

Most of the time, experiments were not intended to provide FMF, and data needed to be extracted and converted to FMF. If numerical experimental data were not directly available in a publication, we digitized the information from the original graphs using WebPlotDigitizer.[42] The original datapoint for D_{UHDR} and the interpolated value of D_{CONV} provided the FMF values, as depicted in the diagram in Figure 1. For interpolation, we used original published fits whenever applicable. Otherwise, we used linear interpolation between the closest datapoints. Experimental uncertainties for FMF (FMF^{upper} and FMF^{lower}) were estimated according to the same procedure, but using the standard error of the mean (upper and lower error bar) of the UHDR data (Fig. 1), if available (data marked with an asterisk in Table 1). We used original datapoints for D_{UHDR} and the interpolated value of D_{CONV} rather than the other way around, because there was a tendency toward more datapoints, a larger data range, and less data fluctuations for CONV data, making interpolation more precise.

No FMF values were obtained for UHDR datapoints if the latter were outside of the data range for the CONV effect, except a few cases for which UHDR datapoints were closely below or above the last CONV datapoint. For these, FMF values were determined either by using the CONV datapoint and interpolating the UHDR data instead or by a short linear extrapolation of CONV data (always <10% in dose). These datapoints are identified in Figure 2. Furthermore, dose levels with no and full effect (ie, below the onset of a measured NTCP threshold and at 100% NTCP) were not considered for the analysis, because dose levels for an isoeffect necessary to derive an FMF value are not uniquely defined for 0% and 100% effect.

As described, isoeffective CONV and UHDR dose levels need to be matched to obtain FMF values (Fig. 1). Of note, this implies that usually data for 2 or more CONV dose levels are necessary for interpolating to an isoeffective UHDR dose level. Consequently, only studies that reported the outcome of an endpoint for multiple dose levels (ie, dose-response studies) generally enabled us to obtain FMF values, and studies using a single dose level usually needed to be excluded because no FMF values could be derived. An exemption worth mentioning were studies for which there was an isoeffective response for the same dose level of UHDR and CONV data.

Data processing, data analysis, and visualization were performed using the R statistical computing language and its libraries.[43] A running average (n = 20) and local second-degree polynomial regression fit (LOESS from R library "stats" with span = 1) was performed to visualize local data averages and general trends as a function of dose.

Parametrization of dose dependence of normal tissue sparing

With the purpose of providing a convenient phenomenological parametrization of the dose dependence of experimental FMF values, we propose a continuous 2-parameter function, and evaluate its capability in describing the data using goodness-of-fit indicators. To date, single- and multifraction in vivo experiments have required large doses per fraction ($\gtrsim$5 Gy) to demonstrate sizable normal tissue sparing by the FLASH effect.[1,3,6,44] Hence, we hypothesize that a minimum threshold dose D_T is needed for the FLASH effect to occur, and that there is consequently no (or a negligibly small) difference in response to CONV and UHDR irradiation for lower doses. NTCP are commonly described by logistic or probit functions as the following[45]:

$$\mathrm{NTCP_X}(D_X)_{D_{50}^X,\gamma_{50}^X} = \frac{1}{1+e^{-\gamma_{50}^X(D_X-D_{50}^X)}} \tag{3}$$

$$\mathrm{NTCP_X}(D_X)_{D_{50}^X,\gamma_{50}^X} = \frac{1}{2}\left(1+\mathrm{erf}\left(\frac{\gamma_{50}^X(D_X-D_{50}^X)}{\sqrt{2}}\right)\right) \tag{4}$$

respectively, where X can be either CONV or UHDR, D_{50}^X is the 50% effect dose threshold, and γ_{50}^X is quantifying the slope at 50% effect. Hence, if one assumes that NTCP dose −response curves are described either by a logistic or a probit curve, both for CONV and UHDR irradiations, for $D > D_T$, one can insert either of the 2 equations into Equation 1. Because both equations depend on the term $\gamma_{50}^X(D_X - D_{50}^X)$, both equations can be rearranged as (see Appendix E1 for a detailed derivation)

$$\mathrm{FMF}(D)_{\mathrm{FMF^{min}},\ D_T} = \begin{cases} 1 \text{ for } D \le D_T \\ (1-\mathrm{FMF^{min}})\dfrac{D_T}{D} + \mathrm{FMF^{min}} \text{ for } D > D_T \end{cases} \tag{5}$$

with the following parameter correspondences for FMF^{min} and D_T for both the logistic and probit models:

$$\mathrm{FMF^{min}} = \frac{\gamma_{50}^{UHDR}}{\gamma_{50}^{CONV}} \text{ and } D_T = \frac{D_{50}^{CONV} - D_{50}^{UHDR} \cdot \frac{\gamma_{50}^{UHDR}}{\gamma_{50}^{CONV}}}{1-\frac{\gamma_{50}^{UHDR}}{\gamma_{50}^{CONV}}} \tag{6}$$

Here, D and D_T both refer to the single fraction UHDR doses. Of note, this behavior corresponds to a sudden effect transition (SET) that is compatible with any phenomenon that causes the radiobiological effectiveness of the deposited

Table 1 Experimental in vivo data comparing normal tissue sparing of UHDR and CONV irradiations analyzed in this work

Identification	References	Biologic system	Endpoint (assessment time)	Oxygenation state	Beam type	Irradiated body part (collimator/ field size)	CONV dose ranges, Gy	UHDR dose range, Gy	CONV TADR, Gy/s	UHDR TADR, Gy/s	UHDR pulse width, μs	UHDR dose per pulse, Gy	UHDR frequency, Hz	UHDR intrapulse dose rate, MGy/s	Total delivery duration, ms
71.1*	Hornsey and Bewley (1971)[27]	Mouse gut	Survival (5 d)	O_2 breathing	e^- 7 MeV	Whole body	8-13	8-17	1	17-83†	2	N/A	400	0.021-0.104‡	100-1000‡
74.1*	Field and Bewley (1974)[28]	Rat skin	Skin reactions (7 d-35 d)§	Physoxic	e^- 7 MeV	Feet	19-31	19-50	0.03, 0.08, 1‖	67, 83	N/A	N/A	N/A	N/A	230-750‡
74.2*,¶	Field and Bewley (1974)[28]	Rat skin	Skin reactions (5 wk-23 wk)§	Physoxic	e^- 7 MeV	Feet	24-31	30-36	0.03,1‖	67	N/A	N/A	N/A	N/A	450-540‡
74.3¶	Field and Bewley (1974)[28]	Rat feet	Deformity (6 mo)	Physoxic	e^- 7 MeV	Feet	24-31	30-36	0.03,1‖	67	N/A	N/A	N/A	N/A	450-540‡
82.1*,¶	Hendry et al (1982)[30]	Mouse tail	Necrosis ND_{50} (7 wk)	Physoxic	e^- 10 MeV	Tail	50-70	50-70	<0.1#	48, 145	0.5-5	1, 3	50	0.6, 1	<4500
14.1	Favaudon et al (2014)[2]	Mouse lung	Average lung reaction score (fibrosis; 24 wk, 36 wk)§	Physoxic	^{137}Cs γ-rays/ e^- 4.5 MeV	Thorax (18 × 20 mm^2)	13-16	17-30	0.03	60	1	<5	100-150	N/A	280-500‡
17.1**	Loo et al (2017)[31]	Mouse gut	Survival LD_{50} (20 d)	Physoxic	e^- 20 MeV	Abdomen (20 mm)	10-22	10-22	0.05	70, 210	N/A	N/A	N/A	N/A	50-310‡
18.1*,¶	Smyth et al (2018)[32]	Mouse whole body	Acute radiation syndrome TD_{50}†† (<60-68 d)	Physoxic	93/124 keV photons	Whole body (Ø100 mm/30 × 100 mm^2)	5.1-10.1	3.6-9.0	0.05	39.1‡‡	N/A	N/A	N/A	N/A	92-230‡
18.2*,¶	Smyth et al (2018)[32]	Mouse gut	Gastrointestinal syndrome TD_{50}†† (<60-68 d)	Physoxic	93/124 keV photons	Abdomen (100 × 60 mm^2/ 30 × 60 mm^2)	7.4-14.8	5.5-13.8	0.06	38.3‡‡	N/A	N/A	N/A	N/A	144-360‡
18.3*,¶	Smyth et al (2018)[32]	Mouse brain	Neurologic symptoms TD_{50}†† (<38 d)	Physoxic	93/124 keV photons	Brain (100 × 30 mm^2/30 × 30 mm^2)	9.8-19.6	7.6-18.9	0.06	41.3	N/A	N/A	N/A	N/A	184-458‡
19.1*	Vozenin et al (2019)[1]	Zebrafish	Fish length (5 d)	21% O_2§§	e^- 6 MeV	Whole body	5-12	5-12	≈0.08	2.8-6.7 × 10^6‡	1.8	5-12	Single pulse	2.8-6.7‡	0.0018
19.2¶,‖‖	Vozenin et al (2019)[4]	Mini pig skin	Skin reactions (7-48 wk)§	Physoxic	e^- 6 MeV	Back (Ø26 mm)	22-34	22-34	≈0.08	220-340	1.8	2.2-3.4	100	1.2-1.9	90
19.3¶	Montay-Gruel et al (2019)[3,8]	Mouse brain	Memory, novel object recognition (2 mo)	Physoxic	e^- 6 MeV	Brain (Ø17 mm)	10	10-14	0.09-0.16‡	5.6-7.8 × 10^6‡	1.8	10-14	Single pulse	5.6-7.8‡	0.0018
19.4*,¶	Beyreuther et al (2019)[33]	Zebrafish	Survival (4 d)	21% O_2§§	p 224 MeV (plateau)	Whole body	10-43	10-43	0.08	100	N/A¶¶	N/A¶¶	N/A	0.0005¶¶	100-430‡
19.5*	Beyreuther et al (2019)[33]	Zebrafish	Pericardial edema (3, 4 d)§	21% O_2§§	p 224 MeV (plateau)	Whole body	10-43	10-43	0.08	100	N/A¶¶	N/A¶¶	N/A	0.0005¶¶	100-430‡
19.6*	Beyreuther et al (2019)[33]	Zebrafish	Spinal curvature (3, 4 d)§	21% O_2§§	p 224 MeV (plateau)	Whole body	10-43	10-43	0.08	100	N/A¶¶	N/A¶¶	N/A	0.0005¶¶	100-430‡
20.1*,¶	Levy et al (2020)[34]	Mouse gut	Crypt survival (96 h)	Physoxic	e^- 16 MeV	Abdomen (30 × 40mm^2)	12-16	12-16	0.079	216	5	2	108	0.4	56-74‡

(*Continued*)

Table 1 (*Continued*)

Identification	References	Biologic system	Endpoint (assessment time)	Oxygenation state	Beam type	Irradiated body part (collimator/ field size)	CONV dose ranges, Gy	UHDR dose range, Gy	CONV TADR, Gy/s	UHDR TADR, Gy/s	UHDR pulse width, μs	UHDR dose per pulse, Gy	UHDR frequency, Hz	UHDR intrapulse dose rate, MGy/s	Total delivery duration, ms
20.2*	Soto et al (2020)[5]	Mouse skin	Skin reactions (8 wk, some earlier)	Physoxic	e^- 16 MeV	Hemithorax ($20 \times 20mm^2$)	10-40	10-40	0.075	180	5	2	90	0.4	56-222‡
20.3¶	Soto et al (2020)[5]	Mouse skin	Survival (50, 100, 150 d)§	Physoxic	e^- 16 MeV	Hemithorax ($20 \times 20mm^2$)	10-40	10-40	0.075	180	5	2	90	0.4	56-222‡
20.4	Zhang et al (2020)[35]	Mouse gut	Survival (9, 12 d)§	Physoxic	p 229 MeV (plateau)	Abdomen (ellipse 16×12 mm^2)	13-22	13-22	0.03-0.08	≈120 (106-138)	0.003¶¶	N/A¶¶	106×10^6	N/A¶¶	96-181
21.1¶	Evans et al (2021)[36]	Mouse gut	Survival LD_{50} (23 d)	Physoxic	p 230 MeV (spread-out Bragg peak)	Abdomen (Ø11 mm)	10-16	10-19	0.1	96 (72-120)	21	0.125‡	756	0.0062	100-200‡
21.2*	Ruan et al (2021)[37]	Mouse gut	Crypt survival in % (3.75 d)§	95% O_2 breathing	e^- 6 MeV	Abdomen (30×33 mm^2)	5-11.8	5-12.5	0.25	$2.2\text{-}5.9 \times 10^6$	3.4	7.5-20	Single pulse	2.2-5.9	0.0034
21.3*,¶	Velalopoulou et al (2021)[38]	Mouse skin	Skin reactions (maximum of 0-8 mo)§	Physoxic	p 230 MeV (plateau)	Leg (20×20 mm^2)	30, 45	30, 45	0.39-0.65	69-124	N/A¶¶	N/A¶¶	N/A	N/A¶¶	240-650‡
21.4¶	Velalopoulou et al (2021)[38]	Mouse skin (soft tissue)	Survival (60 d)	Physoxic	p 230 MeV (plateau)	Leg (20×20 mm^2)	30, 45	30, 45	0.39-0.65	69-124	N/A¶¶	N/A¶¶	N/A	N/A¶¶	240-650‡
21.5*,¶,**	Ollivier et al (2021)[39]	Zebrafish	Fish length (5 d)	21% O_2§§	e^- 6 MeV	Whole body	8.1-11.2	7.9-10.8	≈0.08	$4.4\text{-}6.0 \times 10^6$	1.8	7.9-10.8	Single pulse	4.4-6.0	0.0018
22.1¶	Gaide et al (2022)[9,40]	Human skin	Skin reactions (0-3 mo, 24 mo)§	Physoxic	e^- 8/6 MeV	Arm (28×27 mm^2/42×34 mm^2)	15	15	0.087	166	1	1.5	100	1.5	90
22.2	Sørensen et al (2022)[41]	Mouse skin	Skin reactions (11-25 d)§	Physoxic	P 244/250 MeV (plateau)##	Feet (20×30 mm^2)	23.2-39.2	31.2-53.5	0.35-0.40	65-92 (132-212 Gy/s PBDR)	N/A***	N/A***	N/A	N/A***	0.35-0.73

Abbreviations: CONV = conventional dose rate; FMF = FLASH-modifying factor; LD_{50} = dose for 50% incidence of mortality; N/A = not available; ND_{50} = dose for 50% incidence of necrosis; PBDR = local pencil beam dose rate for 95% dose; TADR = time-averaged dose rate; TD_{50} = dose for 50% incidence of specified toxicity; UHDR = ultra-high dose rate.

* Experimental uncertainties for FMF values were estimated.

† Data series includes data acquired with mixture of TADR between 17 and 83 Gy/s, and contains some datapoints obtained below inclusion TADR threshold of 40 Gy/s. However, these data were included because all UHDR datapoints for 17 to 83 Gy/s are well described by a single normal tissue complication probabilities curve, and no change of effect can be inferred in the range of 17 to 83 Gy/s for this experimental setup.

‡ Value deduced/estimated based on other beam parameters.

§ Pooling multiple endpoints/assessment times.

‖ FMF values were obtained using both CONV dose rates 0.03 and 1 as reference, where applicable.

¶ Data from which only 3 or less FMF values were obtained.

FMF values were obtained by averaging CONV dose levels <0.1 Gy/s.

** Data from study that was not peer-reviewed.

†† Specific toxicity endpoints were severe (15%-20%) weight loss compared with pre-experimental weight and signs of poor well-being (severe diarrhea, moribund behavior, hunched posture, lack of grooming), decline in activity levels, appetite/water intake, and abnormal neurologic signs (seizures, fitting, ataxia, balance disorders).

‡‡ FMF value included because TADR for the irradiation setup was only slightly <40 Gy/s and other data from the same study were included, because they were obtained with a TADR slightly >40 Gy/s.

§§ Oxygen concentration of fish egg medium upon sealing.

‖‖ Data only allowed for estimation of one-sided limit of FMF ≤0.74. FMF of 0.74 was assumed in this work as a conservative estimate.

¶¶ IBA Proteus Plus (Louvain-La-Neuve, Belgium) C230 Cyclotron.

Scanned beam.

*** ProBeam (Varian Medical Systems, Palo Alto, CA).

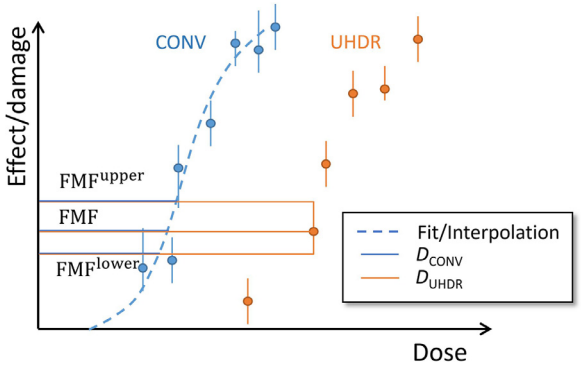

Fig. 1. Conversion of dose-effect data to FLASH-modifying factor (FMF) values for in vivo data. Datapoints were used for ultrahigh dose rates (D_{UHDR}), and interpolated values for conventional dose rates (D_{CONV}). Uncertainties for FMF values (FMF^{upper} and FMF^{lower}) were obtained according to the same procedure but using the upper and lower error bar for the UHDR data, if available.

dose beyond D_T to change (suddenly) from 1 to a reduced constant value of $FMF^{min} < 1$ (ie, any additional damage caused by doses above D_T has a constant reduced additional effect of FMF^{min}). Because the SET function (Eqn. 5) is inversely proportional to dose D for $D > D_T$ and constant below, a piecewise linear behavior is implied for FMF-weighted dose D_{FMF} as a function of dose D. Last, this form implies that (1) if the slopes γ_{50}^{UHDR} and γ_{50}^{CONV} of the NTCP dose–response curves are equal, then $D_T \to \pm\infty$; (2) $\gamma_{50}^{UHDR} < \gamma_{50}^{CONV}$ is a necessary requirement so that $FMF^{min} < 1$; and (3) the NTCP slope ratio $\frac{\gamma_{50}^{UHDR}}{\gamma_{50}^{CONV}}$ defines the minimum FMF that can be reached for high doses. Of note, shallower NTCP slopes for UHDR compared with CONV irradiation were observed experimentally, for instance, by Hornsey and Bewley.[27]

We performed nonlinear regression using the SET function to fit experimental FMF values as a function of dose, and obtained parameter estimates and goodness-of-fit indicators. All regressions and analyses were performed using the R statistical computing language and its libraries.[43] The 95% confidence intervals (CIs) and 95% prediction intervals (PIs) of the fits were obtained using an augmented covariance matrix and Monte Carlo sampling (R library "propagate").

Individual data series

We evaluated the capability of the SET function to fit individual experimental data series with 4 or more FMF values (Tables 1 and 2). For this purpose, we excluded data from Beyreuther et al[33] because they reported mostly negative results with FMF values not significantly different from 1 (Fig. E1). We performed a nonlinear regression of the SET function to obtain parameter estimates for D_T and FMF^{min} and the residual standard deviation σ. The SET function is piecewise linear when multiplied with dose; thus, we also report the coefficient of determination R^2 as an additional indication of the goodness-of-fit for data represented as $D_{FMF} = FMF \cdot D$ versus D using only data with $D > D_T$. If FMF uncertainties were available, we evaluated the aforementioned quantities using a weighted fit of the data with relative

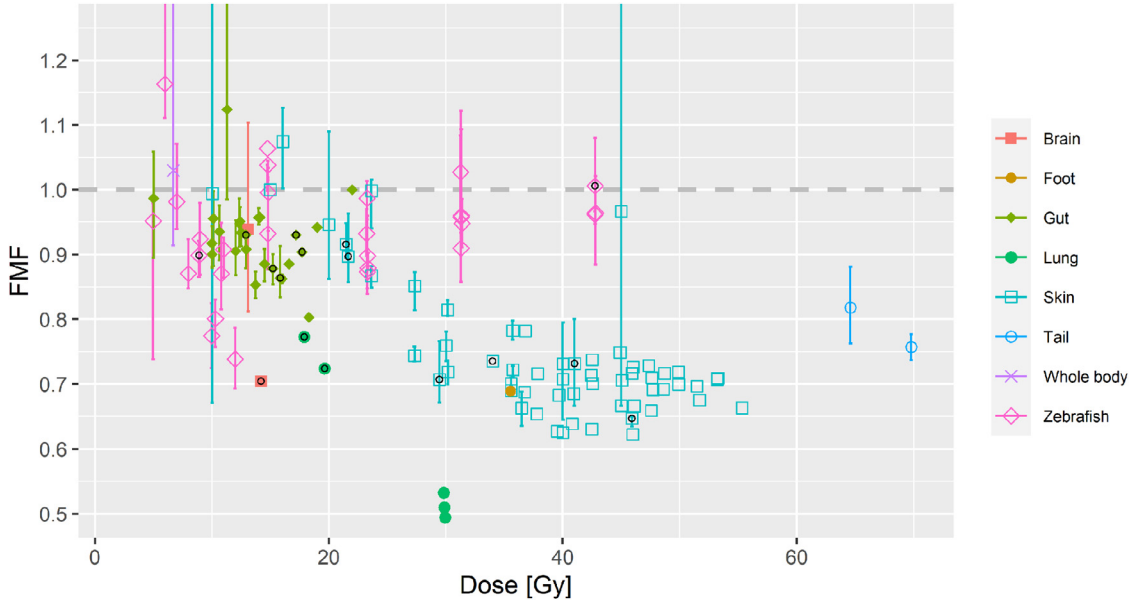

Fig. 2. FLASH-modifying factor (FMF) values of normal tissues as a function of single-fraction ultra-high dose rate dose, grouped by species and organ/body region (ie, mouse brain, rat foot, mouse gut, mouse lung, mammalian skin, mouse tail, mouse whole body, and zebrafish whole body). Datapoints obtained by small extrapolation of conventional dose rate data or interpolating ultra-high dose rate data are indicated by black open circles. (For interpretation of the references to colour in this figure legend, the reader is referred to the web version of this article.)

Table 2 Parameter estimations of D_T and FMF^{min}, their standard uncertainties, and residual standard deviation σ obtained from nonlinear regression to individual and pooled data series using the SET function (Eqn. 5)

Identification/data pool	*n*	D_T, Gy	FMF^{min}	σ	R^2	Avg. FMF <10 Gy	Avg. FMF 10-25 Gy	Avg. FMF >25 Gy
Individual data series								
71.1	9	8.6 ± 1.1	0.70 ± 0.07	0.0078	0.966			
74.1	13	17.9 ± 1.4	0.43 ± 0.05	0.0114	0.743			
14.1	5	13.4 ± 0.4	0.12 ± 0.03	0.0155	0.766			
19.1	8 (6)	6.0 ± 1.7	0.65 ± 0.17	0.0282	0.642			
20.2	5 (3)	16.3 ± 3.8	0.48 ± 0.14	0.0158	0.947			
20.4	4	0.0 ± 90.8	0.94 ± 0.27	0.0497	0.914			
21.2	5	0.0 ± 9.0	0.93 ± 0.06	0.0120	0.991			
22.2	31	0.0 ± 8.6	0.69 ± 0.06	0.0372	0.841			
Pooled data								
All data	123 (115)	9.6 ± 0.8	0.67 ± 0.02	0.1087	0.884	0.95 ± 0.11	0.92 ± 0.08	0.73 ± 0.11
Mammalian	95 (88)	11.3 ± 0.7	0.60 ± 0.02	0.0846	0.913	1.01 ± 0.03	0.92 ± 0.08	0.70 ± 0.07
Mammalian skin	59 (56)	16.6 ± 1.3	0.51 ± 0.03	0.0590	0.807	N/A	0.96 ± 0.07	0.71 ± 0.06
Mammalian without skin	36 (34)	9.9 ± 0.9	0.60 ± 0.05	0.1047	0.897	1.01 ± 0.03	0.90 ± 0.08	0.63 ± 0.14
Mouse gut	25 (24)	6.7 ± 2.7	0.85 ± 0.06	0.0585	0.908	0.99 ± N/A	0.92 ± 0.06	N/A

Abbreviations: Avg. = average; FMF = FLASH-modifying factor; N/A = not available. R^2 was obtained for data, and predictions are represented as D_{FMF} versus D for doses larger than D_T. n is the number of observations. The number of observations above D_T is indicated in the same column by the value in parentheses, in case it was reduced. For pooled data, FMF averages and their corresponding standard deviations are provided for 3 different dose regions.

weights defined by $w = (FMF^{upper} - FMF^{lower})^{-2}$. A fit with equally weighted data was performed otherwise.

Pooled data

We pooled the data by different categories containing a substantial amount of data to evaluate averaged FMF values for the single fraction dose regions <10 Gy, 10 to 25 Gy, and >25 Gy, and obtain parametrizations as a function of dose together with associated uncertainty intervals using the SET function. For this purpose, we evaluated the pooled data groups (Table 1, third column): all data, mammalian data, mammalian skin data (including skin reactions and survival based on euthanasia due to skin reactions), mammalian data without skin data, and mouse gut data (including survival and crypt survival). Nonlinear regression and its evaluation were performed as described herein. The pooled data contains FMF values with and without FMF uncertainties; therefore, pooled fits were obtained using equally weighted data.

Results

Derivation of FMF from experimental data

Figure 2 summarizes the experimental evidence gathered regarding the magnitude of normal tissue sparing provided by the FLASH effect, quantified by FMF, as a function of single-fraction dose and grouped by species and organ/body region (ie, mouse brain, rat foot, mouse gut, mouse lung, mammalian skin, mouse tail, mouse whole body, and zebrafish whole body). The same data grouped by study is shown in Figure E1. Of note, these FMF values were derived independently from any assumptions on the modeling and parametrization of the FLASH effect.

The cumulated experimental FMF values highlight the general trend toward smaller FMF values (ie, a larger sparing effect) for higher doses. This trend is visualized in Figure E1 by a running average and the LOESS regression to the data, which offers a smoothed average of the running average. The figures show that FMF values exhibit a considerable spread of the individual experiments, and some data emerge as outliers of the observed average FMF values. Averages and standard deviations of FMF values in dose regions between 5 and 10 Gy, 10 and 25 Gy, and >25 Gy are provided in Table 2 for the pooled data groups.

Pooled mammalian data and pooled mammalian skin data are displayed in Figure 3. Select data series from single experiments with 4 or more datapoints are displayed in Figure 4 as a function of D_{FMF} versus single fraction dose D. Most of the individual data series show a consistent trend of monotonic decreasing FMF values for larger doses, but the data series by Zhang et al,[35] Ruan et al,[37] and Velalopoulou et al[38] on mouse skin suggest partially an inverse trend.

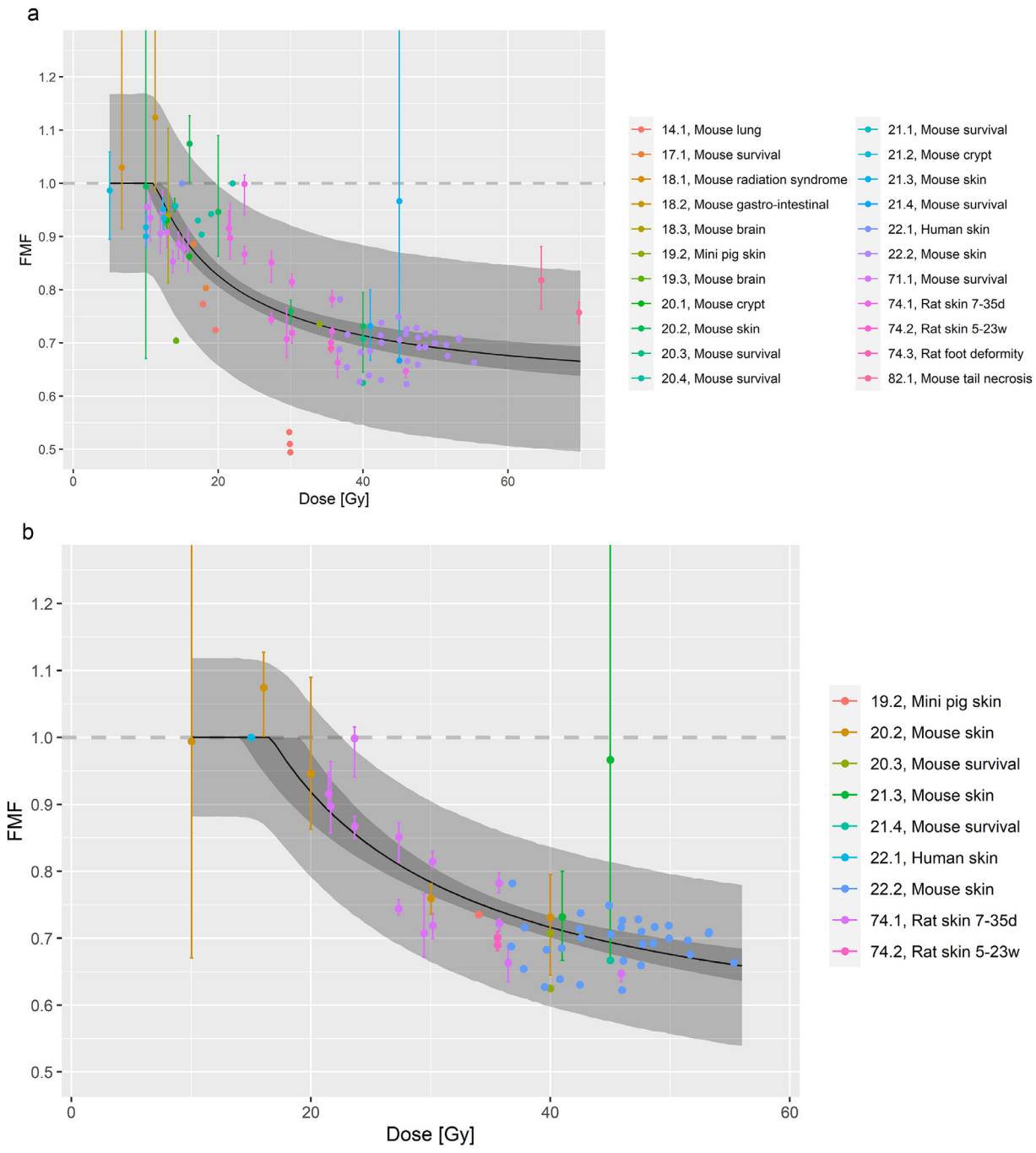

Fig. 3. Pooled mammalian data (top) and pooled mammalian skin data (bottom) by identification, plotted as FLASH-modifying factor (FMF) versus single-fraction ultra-high dose rate dose. A regression to the data using the sudden effect transition (SET) function is shown (solid line) with the 95% prediction interval (light gray band) and 95% confidence interval (dark gray band). (For interpretation of the references to colour in this figure legend, the reader is referred to the web version of this article.)

However, FMF values from these series have considerable uncertainties. For instance, data from Zhang et al is based on an assay with 5 mice per group,[35] and for data from Velalopoulou et al, the skin reaction score started to saturate at 45 Gy.[38] In the series by Ruan et al, the FLASH irradiations were performed under some level of hyperoxygenation.[37]

Parametrizations of individual data series and pooled data

Figure 4 shows that most individual FMF data sets can be parametrized by the SET function when expressed as D_{FMF} versus D. This is corroborated quantitatively by the goodness-of-fit indicators σ and R^2 (Table 2).

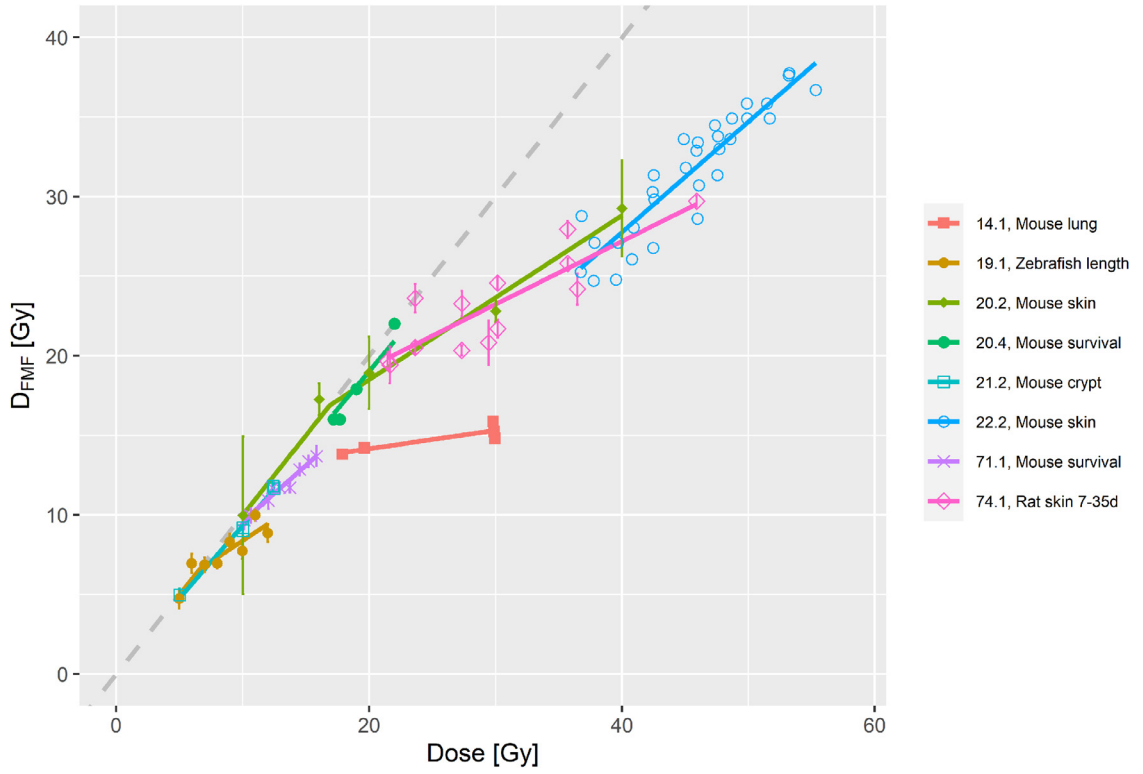

Fig. 4. Experimental data series from in vivo experiments with more than 3 observations, plotted as D_{FMF} = FMF × D versus single-fraction ultra-high dose rate dose D. This representation allows for a visual assessment of the (piecewise) linearity of the individual data series. Fits of the sudden effect transition (SET) function to individual data series with equal weights are shown as solid lines. An FMF of 1 (D_{FMF} = D) is indicated by the gray dashed line. *Abbreviation:* FMF = FLASH-modifying factor. (For interpretation of the references to colour in this figure legend, the reader is referred to the web version of this article.)

Fits of the SET function to pooled mammalian data and mammalian skin data are shown in Figure 3, together with their 95% CI and 95% PI. SET fit parameters, σ, and R^2 are provided in Table 2 for all pooled data groups.

Discussion

Magnitudes and general trends of experimental data

Assuming an isoefficacy in tumor control, the achievable magnitude of normal tissue sparing for clinical scenarios will be pivotal for the added value of FLASH RT using UHDR. Hence, the achievable magnitude of normal tissue sparing needs to be assessed, modelled, and optimized based on available experimental evidence. In this work, we gathered currently available experimental data of normal tissue sparing from in vivo studies performed with single-dose irradiation of small volumes (using field sizes of 2-4 cm at most) for clinically relevant endpoints, and converted them to a common scale using FMF. We are not aware of other works that attempt a systematic evaluation of the dose dependency and magnitude of normal tissue sparing by the FLASH effect based of isoeffect dose ratios derived from gathered experimental data.

For the single data series and pooled data groups, there is generally a trend toward increased normal tissue sparing (ie, a smaller FMF) for larger single-fraction doses. This trend suggests that treatments with large fraction doses should be used to increase normal tissue sparing provided by the FLASH effect. For single-fraction doses <10 Gy, all FMF values of Figure 2 are >0.85, with an average of 0.95 ± 0.11 (Table 2). From a clinical perspective, this implies that, based on the experimental evidence from preclinical single-fraction animal studies in small tissue volumes gathered in this work, a 5% normal tissue sparing by the FLASH effect in terms of dose can be expected on average in this dose region.

The magnitude of FMF values and single-fraction dose ranges for which FMF values can be derived are specific to the biologic system and endpoint. For instance, FMF values for mouse gut are predominantly in the dose range between 10 and 25 Gy, with an average FMF of 0.92 ± 0.06. Instead, data for mammalian skin span a dose range between 10 and 60 Gy, with FMF averages of 0.96 ± 0.07 and 0.71 ± 0.06 for dose ranges of 10 to 25 Gy and >25 Gy, respectively. This means that FMF averages are relatively consistent between the gut and skin, in the range of 10 to 25 Gy, but

above 25 Gy, there is only data for the skin. Remarkably, in the dose region above 25 Gy, similar FMF values of approximately 0.70 were obtained for both electron[5,28] and proton[41] skin irradiations.

Normal tissue sparing magnitudes of ≥20% are often referred to in the literature as a figure of merit for normal tissue sparing by the FLASH effect.[1,6] However, data analyzed in this work indicate that most experimental studies show lower sparing magnitudes for single-fraction doses <25 Gy, and doses >25 Gy were needed by most experimental studies to obtain sparing magnitudes >20% (ie, FMF <0.80). Extremely hypofractionated treatment regimens with ≥25 Gy per fraction are likely to be of interest for a limited range of clinical indications, because they prove often unsuitable to be used in large volumes where most unmet clinical needs of RT are. Furthermore, when delivering modern RT, critical normal tissues are usually already efficiently spared by steep dose gradients and mostly receive doses significantly below the prescribed dose. Hence, such lower normal tissue doses may also decrease normal tissues sparing provided by the FLASH effect.

Therefore, the potential for additional sparing by the FLASH effect will likely be the largest for tissue volumes adjacent to the tumor, which are in the high dose region (eg, in the margin of the planning target volume). In particular, neurocognitive endpoints of the mouse brain[3,8] and mouse lung reactions[2] exhibited larger normal tissue sparing of >20% (FMF <0.8) for single-fraction doses <25 Gy, and these data could point to tissues where a large therapeutic gain could be accomplished for lower doses. However, corresponding FMF values are outliers derived from 2 single experimental studies. Consequently, the reproducibility and robustness of the FMF magnitudes derived from these studies must still be corroborated by further experiments.

The analyzed data are compatible with a minimum dose threshold for significant normal tissue sparing to appear, because available data tend toward an FMF of 1.0 for a decreasing dose (Figs. 2 and 4). However, because of a lack of experimental data, we do not have FMF values for single doses <5 Gy. This lack is mostly owed to the fact that hardly any clinically relevant normal tissue complications arise for such low single-fraction doses and FMF values are consequently not well defined, because NTCP is zero. Fractionated studies may be more appropriate to assess the existence of significant in vivo normal tissue sparing by the FLASH effect for the lower-dose region of 1 to 10 Gy per fraction.

A better understanding of the behavior and magnitude of the FLASH effect for fractionated treatments is also generally of paramount importance for clinical translation. A recent study reported the existence of a normal tissue sparing effect for fractionated UHDR compared with CONV irradiations of the murine brain, but did not find a sparing effect for 4 × 3.5 Gy.[44] Another study[46] reported no normal tissue sparing for cardiac and splenic models of lymphopenia and gastrointestinal syndrome for fraction doses down to 1 and 2 Gy per fraction, but used relatively low TADRs of 36 Gy per second that are likely suboptimal to achieve a pronounced FLASH effect.[7]

Parametrizations of individual data series

Individual data series can be parametrized by the SET function (Eqn. 5, Fig. 4, Table 2), which implies that the analyzed experimental data are compatible with a phenomenon that results in constantly reduced additional normal tissue damage (parametrized by FMF^{min}) for all UHDR doses administered beyond D_T. This is one of the simplest behaviors of FMF as a function of dose, which incorporates a minimum dose threshold D_T while avoiding discontinuities and a hormesis effect. The assumption of a sudden transition, inherent to the SET function, is simplistic, and we anticipate that a gradual transition between the 2 response regions will eventually result in a better description of future experimental data. This means that the adequacy of the SET function to describe the dose response should be reexamined, specifically in the D_T transition region, once more high quality FMF data for extended dose ranges become available.

However, in the meantime, the SET function can be regarded as sufficient to capture the general behavior of the currently available experimental data series, given their data spread and statistical uncertainties, and their mostly limited dose ranges. Additionally, the convenience and advantage of the SET function is its simple, linearizable, 2-free-parameter relation with an increased fitting robustness compared with 3 or more free parameter relations (eg, sigmoidal curves), and that it can be derived using the assumption of a sigmoidal NTCP response beyond D_T. Of note, the experimentally observed dose dependency (ie, a dependency that can be described by the SET function, but potentially with a gradual transition region) is in agreement with the one observed by in vitro cell experiments[47,48] and compatible with the dose dependency expected from radiolytic oxygen consumption.[16-18]

Parametrizations of pooled data

The FMF of the pooled mammalian skin data follow a consistent general trend as a function of single-fraction dose that can be parametrized by the SET function (Fig. 3 [bottom], Table 2). The skin data show an onset of the FLASH effect for doses of approximately 20 Gy, and reach an FMF of approximately 0.70 only for high doses of 30 to 50 Gy. Mammalian skin data generally exhibit normal tissue sparing that manifests only at larger doses compared with other mammalian data, which start to show tissue sparing already for lower doses of approximately 10 Gy (Fig. 3 [top], Table 2). The obtained parameterizations and their associated CIs and PIs highlight the large variability of the experimentally observed onset and magnitude of the FLASH normal tissue sparing effect. As previously mentioned, a

significant data variability is expected because we pooled data obtained from different beams (particle type and energy spectra) with varying temporal dose delivery characteristics, as well as data from different biologic systems (species, tissues, oxygenation states) and endpoints (including late and early reactions).

Additional considerations and limitations

Several limitations and assumptions should be considered when interpreting the results obtained in this work. Experimental studies used for this analysis were not always designed to provide accurate dose−response curves and facilitate the extraction of FMF values via isoeffect levels. Consequently, sometimes only a few datapoints with significant uncertainties were available as a function of dose, which may have led to considerable uncertainties in the derived FMF values. Furthermore, in dose regions where the dose response is shallow, a small variation of the isoeffect level may lead to a large variation of dose and derived FMF values.

The observed sparing magnitudes may relate to an intrinsic property of the investigated biologic systems and endpoints. However, analyzed FMF values originate mostly from initial explorative experimental studies and for some analyzed experiments, a suboptimal normal tissue sparing effect can be expected due to the employed temporal irradiation parameters. Temporal dose delivery parameters vary notably for both CONV and UHDR irradiations between the different data series examined herein, and vary even within individual data series because different temporal delivery parameters, such as total delivery duration or TADRs, were used to vary the delivered dose for different datapoints within a measurement series. Even though we found various reported temporal delivery parameters (Table 1), we focused this study on dose dependency to increase the statistics of our evaluation.

Furthermore, we used a TADR of 40 Gy per second as an inclusion criterium for UHDR irradiations, because such a value was found to produce a pronounced FLASH effect for some experiments and this value is the most commonly referred to in the literature.[1,7,24] However, a precise TADR value is not yet established and may actually vary depending on irradiation conditions and biologic system. Experimental studies report different onset and saturation regions of normal tissue sparing as a function of TADR, ranging between <10 Gy per second, 20 Gy per second, and 280 Gy per second for onset and between 10 Gy per second, 60 Gy per second, 100 Gy per second, and >280 Gy per second for saturation of the FLASH effect.[7,24,30,37,49] These studies clearly demonstrate a dose-rate dependency of the FLASH effect and suggest, in part, a sigmoidal behavior with an upper TADR saturation threshold, but additional experimental studies are needed to understand and quantify this dependency in more detail and disentangle the dependency from other possible dependencies on beam type and temporal dose delivery parameters, as well as other possible dependencies on the biologic system. In summary, even though most FMF values analyzed in this work were obtained from UHDR irradiations with TADRs of ≥60 Gy per second (Table 1), some FMF values may be representative of a TADR region where the FLASH effect is still increasing.

In addition to the spread of FMF values, the pooled parametrizations and averages obtained for a given dose range in this work were often determined only by a few FMF values, mostly originating from only a single or a few experiments. Hence, significant systematic uncertainties may be expected, and averages and parametrizations may be biased toward certain experiments and endpoints by data frequency.

Finally, data presented in the literature about the FLASH effect for normal tissue reactions are exclusively related to small irradiated volumes, and all normal tissue data were obtained for single-fraction experiments. For this reason, our analysis cannot examine how the FLASH effect in vivo behaves for large volumes and/or multiple fractions. A study[44] that was designed to assess the behavior of the FLASH effect for fractionated treatments of mice concluded that "FLASH-RT delivered with hypofractionated regimens is able to spare the normal brain" but does not enable any quantitative conclusions in terms of FMF.

Conclusions

We established a phenomenological description of the FLASH effect in normal tissue as a function of single-fraction UHDR dose using the SET function, which is compatible with currently available experimental findings and implies an increasing sparing effect for an increasing dose and a piecewise linear response behavior when expressed as D_{FMF} versus D. Parameterizations of combined FMF data provide a means to assess expected toxicities for doses delivered with FLASH RT compared with doses delivered with CONV RT while providing uncertainty margins based on data. This may help guide experimental and clinical trial designs and may enable exploratory treatment planning studies that factor in the FLASH effect. At the same time, the data and parametrizations we gathered should prove a useful benchmark for future modeling attempts of the FLASH effect.

Preclinical data gathered in this study evidence normal tissue sparing of 5% on average (in terms of dose) for single-fraction doses <10 Gy, and that the sparing magnitude of the FLASH effect depends on the type of irradiated normal tissue and generally increases with increasing single-fraction dose. The amplitude differences in sparing by the FLASH effect with dose and for different normal tissue systems could have an effect in the choice of indications for the clinical transfer of FLASH RT. With regard to optimized clinical translation, the analyzed data underline the need for further preclinical studies that focus on optimizing and defining beam irradiation parameters to achieve a maximal normal tissues sparing, as well as evaluating the achievable normal tissue sparing magnitude with dose−response curves for clinically relevant organs, endpoints, doses, and fractionation regimens.

References

1. Vozenin MC, Hendry JH, Limoli CL. Biological benefits of ultra-high dose rate FLASH radiotherapy: Sleeping Beauty awoken. *Clin Oncol* 2019;31:407–415.
2. Favaudon V, Caplier L, Monceau V, et al. Ultrahigh dose-rate FLASH irradiation increases the differential response between normal and tumor tissue in mice. *Sci Transl Med* 2014;6:245ra93.
3. Bourhis J, Montay-Gruel P, Gonçalves Jorge P, et al. Clinical translation of FLASH radiotherapy: Why and how? *Radiother Oncol* 2019;139:11–17.
4. Vozenin MC, De Fornel P, Petersson K, et al. The advantage of FLASH radiotherapy confirmed in mini-pig and cat-cancer patients. *Clin Cancer Res* 2019;25:35–42.
5. Soto LA, Casey KM, Wang J, et al. FLASH irradiation results in reduced severe skin toxicity compared to conventional-dose-rate irradiation. *Radiat Res* 2020;194:618–624.
6. Wilson JD, Hammond EM, Higgins GS, Petersson K. Ultra-high dose rate (FLASH) radiotherapy: Silver bullet or fool's gold? *Front Oncol* 2020;9:1563.
7. Montay-Gruel P, Petersson K, Jaccard M, et al. Irradiation in a flash: Unique sparing of memory in mice after whole brain irradiation with dose rates above 100 Gy/s. *Radiother Oncol* 2017;124:365–369.
8. Montay-Gruel P, Acharya MM, Petersson K, et al. Long-term neurocognitive benefits of FLASH radiotherapy driven by reduced reactive oxygen species. *Proc Natl Acad Sci U S A* 2019;166:10943–10951.
9. Bourhis J, Sozzi WJ, Gonçalves Jorge P, et al. Treatment of a first patient with FLASH-radiotherapy. *Radiother Oncol* 2019;139:18–22.
10. van de Water S, Safai S, Schippers JM, Weber DC, Lomax AJ. Towards FLASH proton therapy: The impact of treatment planning and machine characteristics on achievable dose rates. *Acta Oncol Madr* 2019;58:1463–1469.
11. van Marlen P, Dahele M, Folkerts M, Abel E, Slotman BJ, Verbakel WFAR. Bringing FLASH to the clinic: Treatment planning considerations for ultrahigh dose-rate proton beams. *Int J Radiat Oncol Biol Phys* 2020;106:621–629.
12. Mazal A, Prezado Y, Ares C, et al. FLASH and minibeams in radiation therapy: The effect of microstructures on time and space and their potential application to protontherapy. *Br J Radiol* 2020;93 20190807.
13. Gao H, Liu J, Lin Y, et al. Simultaneous dose and dose rate optimization (SDDRO) of the FLASH effect for pencil-beam-scanning proton therapy. *Med Phys* 2022;49:2014–2025.
14. Zhou G. Mechanisms underlying FLASH radiotherapy, a novel way to enlarge the differential responses to ionizing radiation between normal and tumor tissues. *Radiat Med Prot* 2020;1:35–40.
15. Wardman P. Radiotherapy using high-intensity pulsed radiation beams (FLASH): A radiation-chemical perspective. *Radiat Res* 2020;194:607–617.
16. Weiss H. An equation for predicting the surviving fraction of cells irradiated with single pulses delivered at ultra-high dose rates. *Radiat Res* 1972;50:441.
17. Pratx G, Kapp DS. A computational model of radiolytic oxygen depletion during FLASH irradiation and its effect on the oxygen enhancement ratio. *Phys Med Biol* 2019;64 185005.
18. Petersson K, Adrian G, Butterworth K, McMahon SJ. A quantitative analysis of the role of oxygen tension in FLASH radiation therapy. *Int J Radiat Oncol Biol Phys* 2020;1–9.
19. Zhou S, Zheng D, Fan Q, et al. Minimum dose rate estimation for pulsed FLASH radiotherapy: A dimensional analysis. *Med Phys* 2020;47:3243–3249.
20. Pratx G, Kapp DS. Ultra-high-dose-rate FLASH irradiation may spare hypoxic stem cell niches in normal tissues. *Int J Radiat Oncol Biol Phys* 2019;105:190–192.
21. Spitz DR, Buettner GR, Petronek MS, et al. An integrated physico-chemical approach for explaining the differential impact of FLASH versus conventional dose rate irradiation on cancer and normal tissue responses. *Radiother Oncol* 2019;139:23–27.
22. Labarbe R, Hotoiu L, Barbier J, Favaudon V. A physicochemical model of reaction kinetics supports peroxyl radical recombination as the main determinant of the FLASH effect. *Radiother Oncol* 2020;153:303–310.
23. Jin JY, Gu A, Wang W, Oleinick NL, Machtay M, Spring Kong FM. Ultra-high dose rate effect on circulating immune cells: A potential mechanism for FLASH effect? *Radiother Oncol* 2020;149:55–62.
24. Kacem H, Almeida A, Cherbuin N, Vozenin MC. Understanding the FLASH effect to unravel the potential of ultra-high dose rate irradiation. *Int J Radiat Oncol Biol Phys* 2021;1–11.
25. International Commission on Radiation Units and Measurements. ICRU Report 93: Prescribing, recording, and reporting light ion beam therapy. *J ICRU* 2019;16.
26. Page MJ, McKenzie JE, Bossuyt PM, et al. The PRISMA 2020 statement: An updated guideline for reporting systematic reviews. *BMJ* 2021;372:n71.
27. Hornsey S, Bewley DK. Hypoxia in mouse intestine induced by electron irradiation at high dose-rates. *Int J Radiat Biol Relat Stud Phys Chem Med* 1971;19:479–483.
28. Field SB, Bewley DK. Effects of dose-rate on the radiation response of rat skin. *Int J Radiat Biol Relat Stud Phys Chem Med* 1974;26:259–267.
29. McKeown SR. Defining normoxia, physoxia and hypoxia in tumours—Implications for treatment response. *Br J Radiol* 2014;87 20130676.
30. Hendry JH, Moore JV, Hodgson BW, Keene JP. The constant low oxygen concentration in all the target cells for mouse tail radionecrosis. *Radiat Res* 1982;92:172.
31. Loo BW, Schuler E, Lartey FM, et al. Delivery of ultra-rapid flash radiation therapy and demonstration of normal tissue sparing after abdominal irradiation of mice. *Int J Radiat Oncol Biol Phys* 2017;98:E16.
32. Smyth LML, Donoghue JF, Ventura JA, et al. Comparative toxicity of synchrotron and conventional radiation therapy based on total and partial body irradiation in a murine model. *Sci Rep* 2018;8:12044.
33. Beyreuther E, Brand M, Hans S, et al. Feasibility of proton FLASH effect tested by zebrafish embryo irradiation. *Radiother Oncol* 2019;139:46–50.
34. Levy K, Natarajan S, Wang J, et al. Abdominal FLASH irradiation reduces radiation-induced gastrointestinal toxicity for the treatment of ovarian cancer in mice. *Sci Rep* 2020;10:21600.
35. Zhang Q, Cascio E, Li C, et al. FLASH investigations using protons: Design of delivery system, preclinical setup and confirmation of FLASH effect with protons in animal systems. *Radiat Res* 2020;194:656–664.
36. Evans T, Cooley J, Wagner M, Yu T, Zwart T. Demonstration of the FLASH effect within the spread-out Bragg peak after abdominal irradiation of mice. *Int J Part Ther* 2021;8:68–75.
37. Ruan JL, Lee C, Wouters S, et al. Irradiation at ultra-high (FLASH) dose rates reduces acute normal tissue toxicity in the mouse gastrointestinal system. *Int J Radiat Oncol Biol Phys* 2021;111:1250–1261.
38. Velalopoulou A, Karagounis IV, Cramer GM, et al. FLASH proton radiotherapy spares normal epithelial and mesenchymal tissues while preserving sarcoma response. *Cancer Res* 2021;81:4808–4821.
39. Ollivier J, Grilj V, Goncalves PJ, et al. Zebrafish embryos: A high-throughput model to characterize beam parameters able to trigger the FLASH effect. *Phys Med* 2022;94:S63.
40. Gaide O, Herrera F, Sozzi WJ, et al. Comparison of ultra-high versus conventional dose rate radiotherapy in a patient with cutaneous lymphoma. *Radiother Oncol* 2022;174:87–91.
41. Singers Sørensen B, Krzysztof Sitarz M, Ankjærgaard C, et al. In vivo validation and tissue sparing factor for acute damage of pencil beam scanning proton FLASH. *Radiother Oncol* 2022;167:109–115.
42. Rohatgi A. Webplotdigitizer: Version 4.5. Available at: https://automeris.io/WebPlotDigitizer. Accessed April 12, 2022.
43. R Core Team. R: A language and environment for statistical computing. Available at: https://www.R-project.org/. Accessed April 12, 2022.
44. Montay-Gruel P, Acharya MM, Gonçalves Jorge P, et al. Hypofractionated FLASH-RT as an effective treatment against glioblastoma that

reduces neurocognitive side effects in mice. *Clin Cancer Res* 2021;27: 775–784.

45. Bentzen M, Tucker SL. Quantifying the position and steepness of radiation dose-response curves. *Int J Radiat Oncol Biol Phys* 1997; 71:531–542.
46. Venkatesulu BP, Sharma A, Pollard-Larkin JM, et al. Ultra high dose rate (35 Gy/sec) radiation does not spare the normal tissue in cardiac and splenic models of lymphopenia and gastrointestinal syndrome. *Sci Rep* 2019;9:17180.
47. Nias AHW, Swallow AJ, Keene JP, Hodgson BW. Effects of pulses of radiation on the survival of mammalian cells. *Br J Radiol* 1969; 42:553.
48. Weiss H, Epp ER, Heslin JM, Ling CC, Santomasso A. Oxygen depletion in cells irradiated at ultra-high dose-rates and at conventional dose-rates. *Int J Radiat Biol Relat Stud Phys Chem Med* 1974;26:17–29.
49. Cunningham S, McCauley S, Vairamani K, et al. FLASH proton pencil beam scanning irradiation minimizes radiation-induced leg contracture and skin toxicity in mice. *Cancers* 2021;13:1012.